Side Chain Entropy and the Activation of Organocobalamins for Carbon−Cobalt Bond Homolysis: Thermolysis of Neopentylcobalamin-*c*-monocarboxylate, -*c*-*N*-methylamide, -*c*-*N*,*N*-dimethylamide, and -*c*-*N*-isopropylamide

Kenneth L. Brown,* Shifa Cheng, and Helder M. Marques†

Department of Chemistry, Box CH, Mississippi State University, Mississippi State, Mississippi 39762

Received September 15, 1994[⊗]

The contribution of *c* side chain rotational motions to the energetics of thermal carbon−cobalt bond homolysis in neopentylcobalamin (NpCbl) has been investigated by studies of NpCbl analogs including the *c*-monocarboxylate, and the *c*-*N*-methyl, *c*-*N*,*N*-dimethyl, and *c*-*N*-isopropyl derivatives. Spectrophotometric kinetic studies of the thermolysis of these NpCbl analogs in neutral aerobic aqueous solution, after correction for the measured amount of base-off species present under these conditions, showed that the enthalpy of activation was essentially constant (28.4 ± 1.1 kcal mol^{-1}) but that the entropy of activation increased with increasing size of the *c*-COX moiety (X = O^-, 16.4 ± 0.4, X = NH_2, 19.3 ± 0.6, X = NHMe, 21.1 ± 0.7, X = NMe_2, 24.8 ± 0.6, and X = NHiPr, 24.9 ± 0.3 cal mol^{-1} K^{-1}). Molecular mechanics calculations showed that the Co−C bond length and the Co−C−C and Co−C−H bond angles were not altered by rotation of the *c* side chain through 360° about the C7−C37 bond, nor were they significantly altered by the increasing steric bulk of the *c* side chain across the series of compounds. However, the net steric strain experienced by the compound upon rotation of the *c* side chain increased monotonically with the steric bulk of the *c*-COX moiety. Thus, the increase in the rate of thermolysis of the NpCbl analogs as the *c* side chain steric bulk is increased is not due to ground state enthalpic destabilization of the carbon−cobalt bond, but to increasing activation entropy, interpreted as being due to increasing restriction of *c* side chain rotation in the ground state which is relieved (or partially relieved) in the transition state for Co−C bond homolysis. These results may be used to estimate that approximately 30−40% of the decrease in the free energy of thermolysis of 5′-deoxyadenosylcobalamin (AdoCbl, coenzyme B_{12}) brought about by enzyme catalysis could possibly be due to enzymatically induced restriction of the ground state rotational freedom of the three upward projecting acetamide side chains. Thus, such a mechanism could be an important contributor to the catalysis of AdoCbl homolysis although it is almost surely not the sole mechanism employed.

Introduction

The means by which 5′-deoxyadenosylcobalamin- (AdoCbl,[1] coenzyme B_{12}-) requiring enzymes catalyze the homolysis of the carbon−cobalt bond of AdoCbl by some 12 orders of magnitude[3] remains an outstanding problem in the chemistry and biochemistry of cobalt corrinoids. While AdoCbl itself undergoes slow thermolysis at elevated temperature, the reaction is complicated by concomitant Co−C bond heterolysis[3] due to the presence of a β oxygen atom in its organic ligand.[3−7] As a result, AdoCbl homolysis has frequently been modeled using organocobalt corrinoids with bulky organic ligands lacking β hydrogens,[8−14] particularly benzyl- and neopentylcobalamin (NpCbl[1]), which undergo thermolysis at convenient rates and with exclusive Co−C bond homolysis.[10,12,13a,13c,13e,14]

Earlier work from our laboratory[13a,b,e] has suggested the possible importance of corrin ring side chain thermal mobility in the entropic activation of such compounds for carbon−cobalt bond homolysis. Thus, the base-off species (in which the axial Bzm[1] nucleotide is uncoordinated and protonated), and analo-

† On sabbatical leave from the University of the Witwatersrand, P. O. Wits, 2050 Johannesburg, South Africa.

⊗ Abstract published in *Advance ACS Abstracts,* April 15, 1995.

(1) (a) IUPAC-IUB nomenclature for the cobalt corrinoids[2] is used throughout. Abbreviations: AdoCbl, 5′-deoxyadenosylcobalamin (coenzyme B_{12}); CNCbl, cyanocobalamin (vitamin B_{12}); RCbl, alkylcobalamin; CN(H_2O)Cbi^+,[1c] monocyanomonoaquacobinamide; $RCbi^+$, alkylcobinamide; Bzm, 5,6-dimethylbenzimidazole; Np, neopentyl; CNCbl-*c*-COO^-, cyanocobalamin-*c*-monocarboxylate; CNCbl-*c*-NHMe, cyanocobalamin-*c*-*N*-methylamide; CNCbl-*c*-NMe_2, cyanocobalamin-*c*-*N*,*N*-dimethylamide; CNCbl-*c*-NHiPr, cyanocobalamin-*c*-*N*-isopropylamide; Np-13-epiCbl, neopentyl-13-epicobalamin; Np-8-epiCbl, neopentyl-8-epicobalamin; NpBr, 1-bromo-2,2-dimethylpropane; HTEMPO, 4-hydroxy-2,2,6,6-tetramethylpiperidinyloxy; Np-HTEMPO, 1-(2,2-dimethylpropoxy)-2,2,6,6-tetramethyl-4-hydroxypiperidine; EDAC, 1-ethyl-3-(3-dimethyl-aminopropyl)carbodiimide hydrochloride. (b) All organocobalt corrinoids discussed in this paper have the organic ligand coordinated in the "upper" (or β) axial position unless explicitly stated otherwise. (c) Monocyanomonoaquacobinamide and all of the *c* side chain derivatives thereof occur as mixtures of two diastereomers, i.e., α-CN-β-(H_2O)Cbi^+ and α-H_2O-β-(CN)Cbi^+.

(2) *Biochemistry* **1974,** *13,* 1555.

(3) (a) Finke, R. G.; Hay, B. P. *Inorg. Chem.* **1984,** *23,* 3041, **1985,** *24,* 1278. (b) Hay, B. P.; Finke, R. G. *J. Am. Chem. Soc.* **1986,** *108,* 4820. (c) Hay, B. P.; Finke, R. G. *J. Am. Chem. Soc.* **1987,** *109,* 8012.

(4) Hogenkamp, H. P. C.; Oikawa, T. G. *J. Biol. Chem.* **1964,** *239,* 1911.

(5) Schrauzer, G. N.; Sibert, J. W. *J. Am. Chem. Soc.* **1970,** *92,* 1022.

(6) (a) Gerards, L. E. H.; Balt, S. *Recl. Trav. Chim. Pays-Bas* **1992,** *111,* 411. (b) Gerards, L. E. H.; Balt, S. *Recl. Trav. Chim. Pays-Bas* **1994,** *113,* 137.

(7) Brown, K. L.; Salmon, L.; Kirby, J. A. *Organometallics* **1992,** *11,* 422.

(8) (a) Grate, J. H.; Schrauzer, G. N. *J. Am. Chem. Soc.* **1979,** *101,* 4601. (b) Schrauzer, G. N.; Grate, J. H. *J. Am. Chem. Soc.* **1981,** *103,* 541.

(9) Chemaly, S. M.; Pratt, J. M. *J. Chem. Soc., Dalton Trans.* **1980,** 2259 and 2274.

(10) Blau, R. J.; Espenson, J. A. *J. Am. Chem. Soc.* **1985,** *107,* 3530.

(11) Nome, F.; Rezende, M. C.; Saboia, C. M.; deSilva, A. C. *Can. J. Chem.* **1987,** *65,* 2095.

(12) Kim, S.-H.; Chen, H. L.; Feilchenfeld, N.; Halpern, J. *J. Am. Chem. Soc.* **1988,** *110,* 3120.

(13) (a) Brown, K. L.; Brooks, H. B. *Inorg. Chem.* **1991,** *30,* 3420. (b) Brown, K. L.; Brooks, H. B.; Behnke, D.; Jacobsen, D. W. *J. Biol. Chem.* **1991,** *266,* 6737. (c) Zou, X.; Brown, K. L. *J. Am. Chem. Soc.* **1993,** *115,* 6689. (d) Brown, K. L.; Evans, D. R. *Inorg. Chem* **1994,** *33,* 6380. (e) Brown, K. L.; Zou, X.; Evans, D. R. *Inorg. Chem* **1994,** *33,* 5713.

(14) Waddington, M. D.; Finke, R. G. *J. Am. Chem. Soc.* **1993,** *115,* 4629.

0020-1669/95/1334-3038$09.00/0

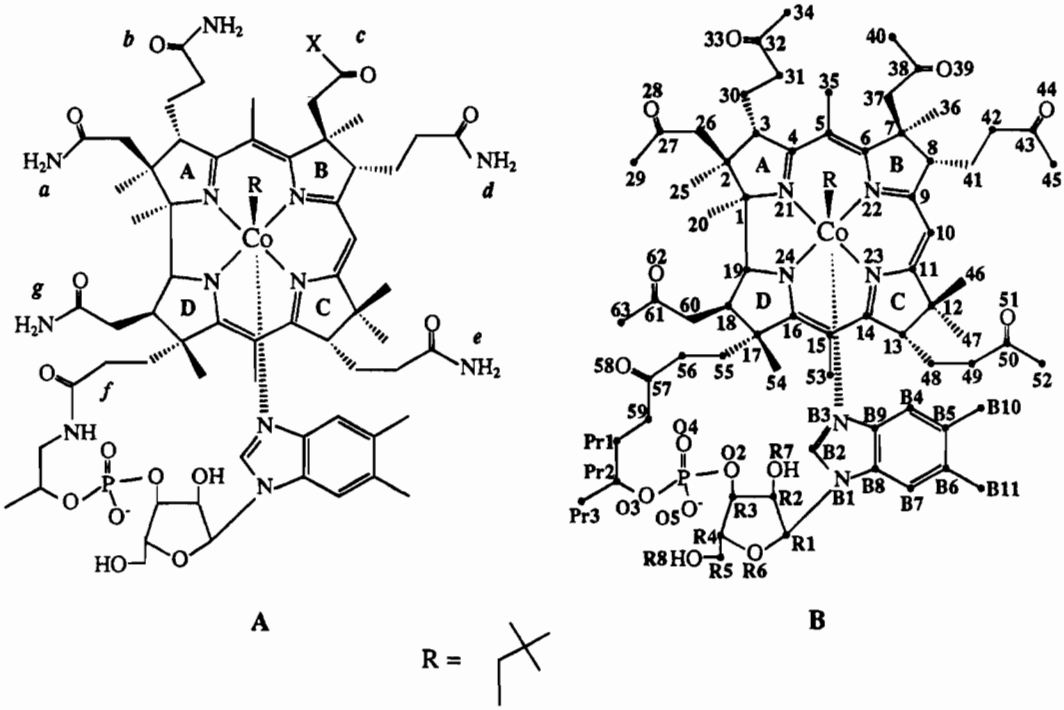

A B

R =

X = O^- NpCbl-*c*-COO^-

X = NH_2 NpCbl

X = $NHCH_3$ NpCbl-*c*-NHMe

X = $N(CH_3)_2$ NpCbl-*c*-NMe_2

X = $NHCH(CH_3)_2$ NpCbl-*c*-NHiPr

Figure 1. Structure (A) and numbering scheme (B) for neopentylcobalamin (NpCbl) and its *c* side chain modified analogs.

gous cobinamides (which lack an axial nucleotide) of such complexes are 2–3 orders of magnitude less reactive than the base-on species,[3c,8b,10,12,13a] a phenomenon known as the "base-on" effect. This reduction in thermal lability for benzyl- and NpCbl has been shown to be due to a large reduction in the (positive) entropy of activation for thermolysis upon removal of the axial ligand.[13a] This observation has led to the hypothesis that the thermal motions of the upward projecting acetamide side chains (Figure 1) are an important source of entropic activation for RCbl thermolysis. In this view, the thermal mobility of the *a*, *c*, and *g* acetamides is significantly restricted in the ground state by the bulky organic ligand. Incipient separation of the organic radical and the Co^{II} complex in the homolysis transition state would thus relieve (or reduce) this restriction on side chain mobility, generating significant entropic activation for Co–C bond cleavage. If, in the base-off (and cobinamide) species, the flexible corrin ring is capable of bending downward,[8b] away from the bulky organic ligand, steric suppression of acetamide side chain thermal motion in the ground state would be considerably lessened. This would result in an increase in the ground state entropy of the base-off (or cobinamide) species and a reduction in the relative increase in entropy as the transition state is approached, compared to the base-on species.

If the entropic effect of acetamide side chain mobility is indeed important in the activation of RCbls for carbon–cobalt bond homolysis, AdoCbl-requiring enzymes could conceivably utilize this effect in order to catalyze the thermolysis of AdoCbl. Thus, an upward flexing of the corrin ring in enzyme-bound AdoCbl, perhaps engendered by hydrogen bonding to the downward projecting *b*, *d*, and *e* propionamides (but *not* to the upward projecting acetamides), would increase the steric restriction to acetamide side chain mobility, thus decreasing the ground state entropy of the AdoCbl-enzyme complex. In order to completely explain an enzymatic rate enhancement of some 10^{12}, approximately 55 cal mol^{-1} K^{-1} of entropic destabilization would be required from such a mechanism.[15] We have consequently undertaken the study described herein to explore the importance of side chain thermal mobility on the entropy of activation for the thermolysis of the model compound NpCbl. Our approach has been to modify the steric bulk of the readily accessible *c* acetamide side chain in order to modify its thermal mobility by altering the steric hindrance to its free rotation by the bulky Np ligand. To this end, we have synthesized and studied the thermolysis of NpCbl analogs including the *c*-monocarboxylate, (NpCbl-*c*-COO^-), the *c*-*N*-methylamide

(15) Finke's[3] calculation of the enzymatic enhancement of AdoCbl homolysis ($\approx 10^{12}$) is for the enzyme ethanolamine deaminase[16] at 25 °C. A similar calculation for the ribonucleotide reductase of *Lactobacillus leichmannii* at 37 °C using Blakley's data[17] gives an enhancement of 5×10^9. This would require an entropic destabilization of about 44 cal mol^{-1} K^{-1} if the enhancement were entirely entropic in nature.

(16) Hollaway, M. R.; White, H. A.; Joblin, K. N.; Johnson, A. W.; Lappert, M. F.; Wallis, O. C. *Eur. J. Biochem.* **1978**, *82*, 143.

(17) (a) Tamao, Y.; Blakley, R. L. *Biochemistry* **1973**, *12*, 24. (b) Orme-Johnson, W. H.; Beinert, H.; Blakley, R. L. *J. Biol. Chem.* **1974**, *249*, 2338.

(NpCbl-*c*-NHMe), the *c*-*N,N*-dimethylamide (NpCbl-*c*-NMe_2), and the *c*-*N*-isopropylamide (NpCbl-*c*-NHiPr). Molecular mechanics calculations strongly suggest that rotation of the *c* side chain is increasingly hindered as the steric bulk of the side chain is increased, and our kinetic analysis demonstrates that the effect of these modifications on carbon−cobalt bond thermolysis is primarily entropic.

Experimental Section

Materials. 1-Bromo-2,2-dimethyl propane (neopentyl bromide, NpBr), 4-hydroxy-2,2,6,6-tetramethylpiperidinyloxy (H-TEMPO), chloramine-T hydrate, methylamine hydrochloride, 1-ethyl-3-(3-(dimethylamino)propyl)carbodiimide hydrochloride, dimethylamine hydrochloride, isopropylamine, cerous nitrate hexahydrate, *N,N*-dimethylformamide, and *N,N*-diisopropylethylamine were from Aldrich. Zinc wool and *O*-(*N*-succinimidyl)-*N,N,N′,N′*-tetramethyluronium tetrafluoroborate were from Fluka. CNCbl was from Roussell.

Cyanocobalamin-*c*-lactone was obtained by a modification[18] of the chloramine-T method of Bonnett, et al.[19]

Cyanocobalamin-*c*-monocarboxylate.[20] CNCbl-*c*-lactone (100 mg, 73.8 μmol) was dissolved in 30 mL of 10% (w/v) aqueous NH_4Cl, and the solution was deoxygenated by argon purging for 60 min. The solution was transferred by cannula to a deaerated flask containing excess zinc wool which had been briefly freshened with 1.0 M HCl and rinsed well with water. After 3 h of continuous argon purge at room temperature, the zinc wool was removed, the pH was adjusted to between 2 and 3 with HCl, and the reaction mixture was desalted on Amberlite XAD-2.[21] The product was purified by semipreparative HPLC[22] (yield, 80 mg, 59.0 μmol, 80%). FAB MS: Calculated for M + H^+ for CNCbl-*c*-COOH, 1357.4; found, 1357.7. The ^{13}C NMR spectrum (Table SI, available as supplemental material) was tentatively assigned by analogy to those of CNCbl[23,24] and CNCbl-*c*-NHMe (vide infra). The absence of the *c* side chain amide was confirmed by ^1H, ^{15}N HMQC NMR spectroscopy, as previously described[24,25] (Table SII, available as supplemental material). Reamidation with NH_4Cl[26] gave CNCbl, as determined by its HPLC retention time and its ^{13}C NMR spectrum.[23,24]

Cyanocobalamin-*c*-*N*-methylamide.[26] CNCbl-*c*-COO^- (100 mg, 73.8 μmol) was dissolved in 40 mL of water and 4.98 g (73.8 mmol) methylamine hydrochloride was added. After the pH was adjusted to between 5 and 6 with 0.1 M KOH, 0.7 g (3.7 mmol) 1-ethyl-3-(3-(dimethylamino)propyl)carbodiimide hydrochloride (EDAC) was added with gentle stirring. The reaction mixture was stirred overnight, desalted on Amberlite XAD-2, and the product purified by semipreparative HPLC (yield, 55.6 mg, 40.6 μmol, 55%). FAB MS: calculated for M + H^+, 1370.4; found, 1370.5. The ^1H and ^{13}C NMR spectra were unambiguously assigned using homonuclear and heteronuclear 2D NMR methods as described previously.[27] A complete correlation table is given in Table SIII, and the ^1H and ^{13}C NMR assignments are given in Table SII, available as supplemental material. The ^1H, ^{15}N HMQC spectrum (Table SII) was readily assignable by analogy to that of CNCbl.[25b]

Cyanocobalamin-*c*-*N,N*-dimethylamide. CNCbl-*c*-NMe_2 was prepared in 51% yield by the same method used for CNCbl-*c*-NHMe, using dimethylamine hydrochloride. FAB MS: calculated for M + H^+, 1384.4; found, 1384.4. ^{13}C and amide ^1H and ^{15}N NMR assignments are given in Tables SI and SII, respectively.

Cyanocobalamin-*c*-*N*-isopropylamide. The EDAC method used for CNCbl-*c*-NHMe and CNCbl-*c*-NMe_2 gave a poor yield (15%). The following procedure[28] gave better results. CNCbl-*c*-COO^- (100 mg, 73.7 μmol) was dissolved in a mixture of dimethylformamide (0.22 mL) and water (0.22 mL). To this solution, 0.038 mL of diisopropylamine and 28 mg of *O*-(*N*-succinimidyl)-*N,N,N′,N′*-tetramethyluronium tetrafluoroborate was added. After 10 min, 0.030 mL of isopropylamine was added. After 10 min more, the reaction mixture was desalted on Amberlite XAD-2 and the product was purified by semipreparative HPLC (yield, 41 mg, 40%). FAB MS: calculated for M + H^+, 1398.5; found, 1398.8. ^{13}C and amide ^1H and ^{15}N NMR assignments are given in Tables SI and SII, respectively.

Cyanoaquacobinamides. The monocyanomonoaquacobinamide derivatives of CNCbl-*c*-COO^-, CNCbl-*c*-NHMe, CNCbl-*c*-NMe_2, and CNCbl-*c*-NHiPr[1c] were prepared by cerous hydroxide catalyzed phosphodiester hydrolysis of the respective cobalamin derivative, essentially by the procedure of Renz.[29] CN(H_2O)Cbi-*c*-COO, yield, 70%. FAB MS: calculated for $M^+ - H_2O$,[30] 1017.2; found, 1016.7. CN(H_2O)-Cbi-*c*-$NHMe^+$, yield, 87%, FAB MS: calculated for $M^+ - H_2O$, 1030.2; found, 1029.8. CN(H_2O)Cbi-*c*-NMe_2^+, yield, 95%, FAB MS: calculated for $M^+ - H_2O$, 1044.2; found, 1043.8. CN(H_2O)Cbi-*c*-$NHiPr^+$, yield 95%, calculated for $M^+ - H_2O$, 1032.2; found, 1031.5. All of these cobinamides were characterized by their ^{13}C NMR spectra of their dicyano derivatives (Table SIV, available as supplemental material) which were tentatively assigned by analogy to the known assignments for $(CN)_2$Cbi.[24]

Neopentylcobalamin-*c*-monocarboxylate. CNCbl-*c*-COO^- (100 mg, 73.7 μmol) was dissolved in 12 mL of 10% (w/v) aqueous NH_4Cl to which 5 mL of methanol had been added. The solution was deoxygenated by argon purge for 1 h, then transferred by cannula to a deaerated flask containing excess zinc wool which had been freshened briefly with 1.0 M HCl and washed well with water. The reduction was allowed to proceed for 1 h during which time the color changed from red to dark brown. In the dark, NpBr (0.70 mL, 5.56 mmol) was injected through a serum stopper and the alkylation was allowed to proceed for 3 h. The solution was then transferred by cannula into 100 mL of 10^{-3} M HCl and the product was kept acidified for the remainder of the workup in order to keep it in the much more stable, base-off form. The solution was loaded onto an Amberlite XAD-2 column which was washed with 400 mL of 10% $CH_3CN/10^{-3}$ M HCl to remove unreacted starting material, then with 30% $CH_3CN/10^{-3}$ M HCl to elute the product which was stored at −20 °C in 10^{-3} M HCl solution. The yield was 90%. NpCbl-*c*-NHMe (yield 94%), NpCbl-*c*-NMe_2 (yield, 95%), and NpCbl-*c*-NHiPr (yield, 40%) were prepared and stored similarly.

Neopentylcobinamide-*c*-monocarboxylate. NpCbi-*c*-COO was obtained from CN(H_2O)-Cbi-*c*-COO by an analogous procedure except that the solvent was 10% aqueous acetic acid. After reduction and alkylation, the reaction mixture was transferred away from the zinc wool by cannula into an empty flask and was allowed to stand under continuous argon purge at room temperature in the dark for 20 h. This allowed the α diastereomer (i. e., α-NpCbi-*c*-COO) which had been formed (as readily detected by analytical HPLC) to thermally isomerize to the β diastereomer[13c] and permitted work-up of excellent yields (here, 80%) of the latter. NpCbi-*c*-$NHMe^+$ (yield, 80%), NpCbi-*c*-NMe_2^+ (yield, 95%), and NpCbi-*c*-$NHiPr^+$ (yield, 42%) were prepared analogously. In the last case, purification was effected by semipreparative HPLC. All of the $NpCbi^+$ derivatives were characterized by their ^{13}C NMR spectra (Table SV, available as supplemental material) which could be readily, if tentatively, assigned by analogy to that of $NpCbi^+$ itself.[32]

(18) Brown, K. L.; Zou, X.; Wu, G.-Z.; Zubkowski, J. D.; Valente, E. J. *Polyhedron*, in press.
(19) Bonnett, R.; Cannon, J. R.; Clarke, U. M.; Johnson, A. W.; Parker, L. F. J.; Smith, E. L.; Todd, A. *J. Chem. Soc.* **1957**, 1158.
(20) Rapp, P.; Oltersdorf, U. *Hoppe-Seyler's Z. Physiol. Chim.* **1973**, *254*, 32.
(21) Brown, K. L.; Hakimi, J. M.; Nuss, D. M.; Montejano, Y. D.; Jacobsen, D. W. *Inorg. Chem.* **1984**, *23*, 1463.
(22) Jacobsen, D. W.; Green, R.; Brown, K. L. *Methods Enzymol.* **1986**, *123*, 14.
(23) Pagano, T. G.; Marzilli, L. G. *Biochemistry* **1988**, *111*, 1484.
(24) Brown, K. L.; Brooks, H. B.; Gupta, B. D.; Victor, M.; Marques, H. M.; Scooby, D. C.; Goux, W. J.; Timkovich, R. *Inorg. Chem.* **1991**, *30*, 3430.
(25) (a) Brown, K. L.; Zou, X. *J. Am. Chem. Soc.* **1993**, *115*, 1478. (b) Brown, K. L.; Evans, D. R. *Inorg. Chem.* **1993**, *32*, 2544.
(26) Toraya, T.; Krodel, E.; Mildvan, A. S.; Abeles, R. H. *Biochemistry* **1979**, *18*, 417.
(27) Brown, K. L.; Zou, X. *J. Am. Chem. Soc.* **1992**, *114*, 9643.
(28) Bannwarth, W.; Knorr, R. *Tetrahedron Lett.* **1991**, *32*, 1157.
(29) Renz, P. *Methods Enzymol.* **1971**, *18C*, 85.
(30) The parent ion of cationic cobinamides in positive ion FAB MS does not contain a proton from the matrix and is pentacoordinate, thus occuring at $M^+ - H_2O$.[3c,7,31]
(31) Brown, K. L.; Evans, D. R. *Inorg. Chem.* **1990**, *29*, 2559.
(32) Brown, K. L.; Evans, D. R. *Polyhedron*, in press.

Methods. Work requiring anaerobic conditions was carried out in a Vacuum Atmospheres glovebox under an atmosphere of argon or nitrogen as previously described.[13e] Analytical and semipreparative HPLC were carried out as described previously.[13d,e] FAB MS was performed as described elsewhere[7] using a *m*-nitrobenzyl alcohol matrix.[33] UV−visible measurements were obtained on a Cary 219 recording spectrophotometer equipped with a thermostatted 5 cell turret. Temperature in both UV−visible and NMR experiments was measured by the use of a calibrated thermistor device as described previously.[13d,e]

Concentrations of cobalt corrinoids were determined by UV−visible spectroscopy after conversion to their dicyano derivatives. For $(CN)_2$Cbl-*c*-NHMe$^-$, $(CN)_2$Cbl-*c*-NMe_2^-, $(CN)_2$Cbl-*c*-NHiPr$^-$, and the analogous cobinamides, the molar absorptivity of the γ band was assumed to be the same as that of $(CN)_2Cbl^-$ ($\epsilon_{368} = 3.04 \times 10^4$ M^{-1} cm^{-1}).[34] However, for the dicyano derivative of the *c*-monocarboxylate ($(CN)_2$Cbl-*c*-COO^{2-}), which has a different charge, the molar absorptivity of the γ band was determined by the method previously described.[13e] The value obtained ($\epsilon_{368} = 2.95 \pm 0.08 \times 10^4$ M^{-1} cm^{-1}) was not significantly different from that for $(CN)_2Cbl^-$.

Np-HTEMPO and *N*-(2,2-dimethylpropylidene)benzeneamine (the Schiff base of pivalaldehyde and aniline) were synthesized as described previously,[13c] and these trapped products of the anaerobic and aerobic thermolysis, respectively, of the NpCbl derivatives were quantitatively determined by GC.[13c,e] The UV−visible spectra of the cobalt(II) derivatives of the *c* side chain modified CNCbls were generated by reduction of the CNCbl analog in formate or with zinc and the observed molar absorptivities were as follows (λ, log ϵ): CNCbl-*c*-COO^-, 472, 3.89; 400, 3.81; 310, 4.39; CNCbl-*c*-NHMe, 472, 3.93; 400, 3.86; 310, 4.48; CNCbl-*c*-NMe_2, 472, 3.98; 400, 3.87; 312, 4.44; CNCbl-*c*-NHiPr, 472, 3.93; 400, 3.87; 308, 4.45. UV−visible quantitation of cob(II)-alamin derivatives resulting from anaerobic thermolysis of NpCbl derivatives in the presence of HTEMPO was carried out in Schlenk cuvettes.[13c,e]

Aerobic thermolysis kinetics of the NpCbl analogs were studied spectrophotometrically as described previously.[13d,e] Samples (in 1.000 cm pathlength quartz cuvettes) contained $(1.0-2.0) \times 10^{-5}$ M NpCbl derivative, 0.1 M potassium phosphate buffer (pH 7.5), and KCl to maintain the ionic strength at 1.0 M. Reactions were initiated by addition of a small volume of a stock solution of the NpCbl derivative to the sample cuvette which had been incubated in the spectrophotometer cell block for at least 30 min and were monitored at 352 nm. Great care was taken to avoid the errors in temperature maintenance and measurement at above-ambient temperatures which have recently been shown[13d] to be responsible for a wide variation in the activation parameters for NpCbl thermolysis reported in the literature.

For each NpCbl analog, four or five independent kinetic measurements were made at each temperature. The data were fitted to an exponential function using a nonlinear least squares routine and the weighted averages of the first-order rate constants at each temperature (k_{obs}) was calculated as described previously.[13d] Activation parameters (both observed, $\Delta H^{\ddagger}_{obs}$ and $\Delta S^{\ddagger}_{obs}$, and corrected for the occurrence of the base-off species of the NpCbl derivatives at neutral pH, $\Delta H^{\ddagger}_{on}$ and $\Delta S^{\ddagger}_{on}$) were determined from Eyring plots. A thorough statistical analysis allowed propagation of the uncertainties in all measured parameters (rate constants, temperatures, and NMR resonance frequencies) into the final activation parameters as described in detail elsewhere.[13d] Kinetic measurements of the anaerobic thermolysis of the NpCbl analogs were carried out in the presence of 1.0×10^{-3} M HTEMPO in 0.1 M potassium phosphate buffer (pH 7.5), ionic strength 1.0 M (KCl), in Schlenck cuvettes prepared in a glovebox. The reactions were monitored at 474 nm and the data were analyzed as described elsewhere.[13e]

Anaerobic NMR samples of the NpCbl and NpCbi$^+$ analogs in D_2O were prepared as described previously[13d,e] and ^{1}H NMR spectra were observed on a GE QE300 NMR spectrometer operating at 300.669 MHz. Temperature was measured and C10 hydrogen resonance frequencies were determined as described previously.[13d,e]

The steric interactions of the *c* side chains of NpCbl, CH_3Cbl, and their *c* side chain modified derivatives were investigated by molecular mechanics (MM) techniques using a modified[35] version of the molecular mechanics program MM2(87)[36] and the force field recently developed[37] specifically for cobalamins. Calculations were performed on an IBM-compatible PC fitted with an Intel 486-dx2 microprocessor. Molecules were constructed and energy-minimized structures viewed using ALCHEMY III (Tripos Associates, St. Louis, MO). The ALCHEMY III-MM2 interface supplied as part of the ALCHEMY III suite was used for setting up the input files to MM2 but, because of the large size of the molecules, the atom connectivity table had to be edited manually. A convergence criterion of <0.002 kcal mol^{-1} between successive iterations was used.

Our recent study[37] of cobalt corrinoids by MM techniques showed that the coordinated Np ligand in NpCbl experiences steric restrictions to free rotation about the Co−C bond and appears to be restricted to a conformation where two of the terminal methyl groups of the Np ligand straddle the C46 methyl substituent of the corrin ring (Figure 1). In the present study, coordinated Np was placed in, but not confined to, this orientation. The consequences of substitution in the *c* side chain were investigated by determining the effect of its rotation about the C7−C37 bond by using the dihedral driver in MM2(87) to drive the C6-C7−C37−C38 torsional angle, ω_1, through 360° in steps of 10° in both a clockwise and counterclockwise direction. Where obvious discontinuities in the strain-energy profile occurred (a consequence of a major structural reorganization in the molecule and an artifact of the dihedral drive method[38]), the resulting structure was used as the starting point for a further program run in which the torsional angle, ω_1, was driven in the opposite direction to that in which the discontinuity occurred. This process was repeated until no further lower energy structures were found. The results reported are for the lowest energy structure found for any given torsional angle, ω_1.

For each energy-minimized structure, the total strain energy, the Co−C bond length, and the Co−C−C and Co−C−H bond angles were recorded. Since the total strain energy in any given calculation depends on the number of atoms in the molecule, a direct comparison of the strain energy of different molecules is not meaningful. The strain energies were therefore recorded as ΔE values relative to the minimum strain energy found in each structure (in all cases, this occurs at $\omega_1 = \pm 180°$, when C37 is vertically above C7 and the *c* side chain points outwards from the molecule). To quantify the total strain energy in each molecule which arises from rotation of the *c* side chain, ΔE values were plotted against ω_1 and the area under the curve, an integrated strain energy, E_{str}, was determined numerically. Assuming that free rotation of the *c* side chain occurs, the greater the average steric strain in the complex during rotation of the side chain, the greater E_{str}. The difference between the integrated strain energy for a given NpCbl derivative and the corresponding CH_3Cbl derivative, ΔE_{str}, is then a measure of the additional strain imposed by the large ligand in the β coordination site in the former complexes.

In order to quantify the steric bulk of the *c* side chain substituents, the van der Waals volume of each substituent was calculated. The structures of $HCOO^-$, $HCOONH_2$, $HCOONHCH_3$, $HCOON(CH_3)_2$, and $HCOONHCH(CH_3)_2$ were energy-minimized using the standard MM2 force field.[36] The carbonyl H atom was then removed and the resulting structure centered at the Cartesian origin. A volume was chosen within which the molecule could be contained, and this volume was subdivided into volume elements which were grid searched to determine whether they fell within the van der Waals radius (sp^3 C, 1.90 Å; sp^2 C, 1.94 Å; sp^2 O, 1.74 Å; amide N, 1.82 Å; and H, 1.50 Å) of any atom in the molecule. Care was taken to ensure that a volume element which fell within the van der Waals radius of more than one atom was counted only once. At the end of the search, the number of volume elements falling within the van der Waals radii of the atoms of the group was tallied and multiplied by the volume of each volume element to yield

(33) (a) Meili, J.; Seibl, J. *Org. Mass Spectrom.* **1984**, *21*, 793. (b) Sharp, T. R.; Santander, P. J.; Scott, A. I. *Tetrahedron Lett.* **1990**, *31*, 6163.
(34) Barker, H. A.; Smyth, R. D.; Weissbach, H.; Toohey, J. I.; Ladd, J. N.; Volcani, B. E. *J. Biol. Chem.* **1960**, *235*, 480.
(35) Munro, O. Q.; Bradley, J. C.; Hancock, R. D.; Marques, H. M.; Marsicano, F.; Wade, P. W. *J. Am. Chem. Soc.* **1992**, *114*, 7218.
(36) (a) Allinger, N. L. *J. Am. Chem. Soc.* **1977**, *99*, 8127. (b) Allinger, N. L.; Yuh, Y. MM2(87), distributed to academic users by QCPE, under special agreement with Molecular Design Ltd., San Leandro, CA.
(37) Marques, H. M.; Brown, K. L. *THEOCHEM*, in press.
(38) Burkert, U.; Allinger, N. L. *J. Comput. Chem.* **1982**, *3*, 40.

the total van der Waals volume of that group. A volume element of 0.001 Å^3, which reproduced the volume of a sphere to better than 0.5%, was used.

Results

Synthesis and Characterization of *c* Side Chain Modified Cobalt Corrinoids. CNCbl-*c*-COO$^-$ is readily available by reduction of CNCbl-*c*-lactone.[18] While reduction of the latter with borohydride gives mixtures of CNCbl-*c*-COO$^-$ and its epimer at C8,[19,22] reduction with zinc in ammonium chloride [22] cleanly gives CNCbl-*c*-COO$^-$ in very good yield. Combined with our previous improvement in the synthesis of CNCbl-*c*-lactone,[18,19] CNCbl-*c*-COO$^-$ may now be obtained in nearly 75% overall yield from CNCbl. This ready availability of CNCbl-*c*-COO$^-$ gives easy access to CNCbl-*c*-*N*-alkylamides by amidation with primary or secondary amides. While use of 1-ethyl-3-(3-(dimethylamino)propyl)carbodiimide[26] as a coupling reagent proved suitable for amidation with methylamine and dimethylamine in moderate yields, the method of Bannwarth and Knorr[28] provided far better yields for amidation with isopropylamine.

The *c* side chain modified CNCbls were characterized by their ^{13}C NMR spectra (Table SI, available as supplemental material) which could be readily, if tentatively, assigned by analogy to the assigned spectrum of CNCbl.[23,24] In order to be certain of the legitimacy of such assignments, the ^{1}H and ^{13}C NMR spectra of CNCbl-*c*-NHMe were unambiguously assigned using 2D homonuclear and heteronuclear NMR methods. A correlation table is given in Table SIII, and the NMR assignments for CNCbl-*c*-NHMe are given in Table SI (available as supplemental material). The *c*-*N*-methyl resonance of CNCbl-*c*-NHMe was observed at 28.7 ppm, those of CNCbl-*c*-NMe$_2$ at 38.3 and 41.1 ppm, and the secondary carbon of the *c*-*N*-isopropyl group was observed at 44.7 ppm, while the isopropyl methyls resonated at 24.06 and 24.14 ppm. In CNCbl-*c*-COO$^-$, the C38 carbonyl and C37 methylene resonances were shifted downfield by 3.1 and 1.7 ppm, respectively, from their locations in CNCbl, similar to the shifts of the carbonyl and adjacent methylene resonances seen in the CNCbl-*b*-, *d*-, and *e*-monocarboxylates.[23,39] In contrast, the C38 resonance was shifted upfield (by 2.4 to 3.5 ppm) from its position in CNCbl in the *c* *N*-alkylated derivatives. The only other significant chemical shift differences between the analogs and CNCbl occurred at C37, C5, C6, C7, C8, and C9.

Confirmation of the *c* side chain alterations in these analogs was obtained by observation of their ^{1}H, ^{15}N HMQC spectra,[24,25] optimized for a one-bond N−H coupling of 90 Hz (Table SII, available as supplemental material). For CNCbl-*c*-COO$^-$ and CNCbl-*c*-NMe$_2$, both the amide ^{1}H and ^{15}N resonances occurred at chemical shifts very close to those previously observed for CNCbl,[25b] but the *c* amide ^{15}N cross-peaks (at 114.4 ppm and 7.01, 7.54 ppm in CNCbl) were missing. In contrast, for CNCbl-*c*-NHMe and CNCbl-*c*-NHiPr, the *c* amide nitrogen resonance, which correlated to only one proton, was shifted upfield to 109.8 ppm in the former, but downfield to 129.9 ppm in the latter. This is strictly analogous to what is seen in *N*-alkylureas[40] and *N*-alkylformamides,[41] where, for instance in the ureas, the *N*-methyl nitrogen is shifted upfield by 7.6 ppm from urea, while the *N*-isopropyl nitrogen is shifted downfield by 31.7 ppm.

The *c* side chain modified CN(H$_2$O)Cbi$^+$ analogs were readily obtained by standard cerous hydroxide catalyzed phosphodiester hydrolysis[29] of the appropriate CNCbl analogs, and were characterized by the ^{13}C NMR spectra of their (CN)$_2$Cbi derivatives. These ^{13}C spectra were tentatively assigned by analogy to the known assignments for (CN)$_2$Cbi itself[24] and the chemical shifts are given in Table SIV (available as supplemental material). The *c* *N*-alkyl ^{13}C resonances occurred at positions virtually identical to those of the CNCbl analogs, the only significant chemical shift differences between these analogs and (CN)$_2$Cbi itself occurring at C38, C37, and C5−C9.

The neopentyl derivatives of the *c* side chain modified Cbls could be obtained by reductive alkylation with NpBr in a manner similar to that previously used for the synthesis of NpCbl and other NpCbl analogs.[8b,13a,d,e,14] Excellent yields were obtained (90−95%) except for NpCbl-*c*-NHiPr which proved more difficult to synthesize (yield, 40%). In the case of the cobinamides, HPLC chromatograms of reductive alkylation reaction mixtures showed clear evidence of the formation of significant amounts of the α-NpCbi$^+$ analog, in which the organic group is in the "lower" axial ligand position, as was previously shown to be the case for NpCbi$^+$ itself.[13c] However, owing to the much greater thermal lability of the α-NpCbi$^+$s than their β diastereomers, incubation of the alkylation reaction mixture (after separation from the zinc reducing agent) under strictly anaerobic conditions overnight permitted complete isomerization of the α diastereomers to the β-NpCbi$^+$s. This allowed preparation of the *c* side chain modified β-NpCbi$^+$s in good yield (80−95%), with the exception of β-NpCbi-*c*-NHiPr$^+$ which could be obtained only in 42% yield.

The *c* side chain modified NpCbi$^+$ analogs were characterized by their ^{13}C NMR spectra (Table SV, available as supplemental material) which again could be tentatively assigned by analogy to the unambiguously assigned ^{13}C NMR spectrum of the NpCbi$^+$ parent.[32] The *c* *N*-alkyl ^{13}C resonances occurred at 28.2 ppm for NpCbi-*c*-NHMe$^+$, 38.1 and 40.7 for NpCbi-*c*-NMe$_2^+$, and 44.0, 24.06, and 24.19 for NpCbi-*c*-NHiPr$^+$. The C38 carbonyl and C37 methylene resonances were shifted from those of the parent compound in an analogous manner to these resonances in the CNCbl analogs. Again, only these two resonances and the C5−C9 resonances were significantly shifted in the NpCbi$^+$ analogs. As was the case with NpCbl, Np-13-epiCbl, and Np-8-epiCbl,[13e,32] both the ^{1}H and ^{13}C NMR spectra of the *c* side chain modified NpCbls were significantly broadened, presumably due to exchange between the base-on and base-off species (vide infra). These derivatives were consequently characterized by analysis of the products of their thermolysis.

Thermolysis Products. The thermolyses of NpCbl,[13a,d,14] α-NpCbl and α-NpCbi$^+$,[13c] and Np-13-epiCbl and Np-8-epiCbl[13e] are now well established to proceed via initial carbon−cobalt bond homolysis to form a caged Np$^\bullet$; Co^{II} pair (Scheme 1). Due to very high rates of recombination of such caged radical pairs[14,42−44] and the inherent stability of the cobalt(II) product under anaerobic conditions (the "persistent radical effect"),[44,45] such complexes are extraordinarily stable under strictly anaerobic conditions in the absence of any radical traps.[46] In the presence of a suitable radical trap, such as HTEMPO, the organic radical can be rapidly trapped, driving the ther-

(39) Marques, H. M.; Scooby, D. C.; Victor, M.; Brown, K. L. *Inorg. Chim. Acta* **1989**, *162*, 151.
(40) Sibi, M. P.; Lichter, R. L. *J. Org. Chem.* **1979**, *44*, 3017.
(41) Nakanishi, H.; Roberts, J. D. *Org. Magn. Reson.* **1981**, *15*, 7.
(42) Endicott, J. F.; Netzel, T. L. *J. Am. Chem. Soc.* **1979**, *101*, 4000.
(43) Chagovetz, A. M.; Grissom, C. B. *J. Am. Chem. Soc.* **1993**, *115*, 12,-152.
(44) Daikh, B. E.; Finke, R. G. *J. Am. Chem. Soc.* **1992**, *114*, 2938.
(45) Fischer, H. *J. Am. Chem. Soc.* **1986**, *108*, 3925.
(46) For an analogous model complex, $C_6H_5CH_2Co^{III}[C_2(DO)DOH)pn]I$ (*trans*-benzyliodo(trimethylenedinitrilo)bis(3-oximato-2-pentanone)-cobalt(III)), Finke's measurements and calculations[44,47] predict that untrapped anaerobic thermolysis will lead to only 0.18% net decomposition after 1000 years.

Scheme 1

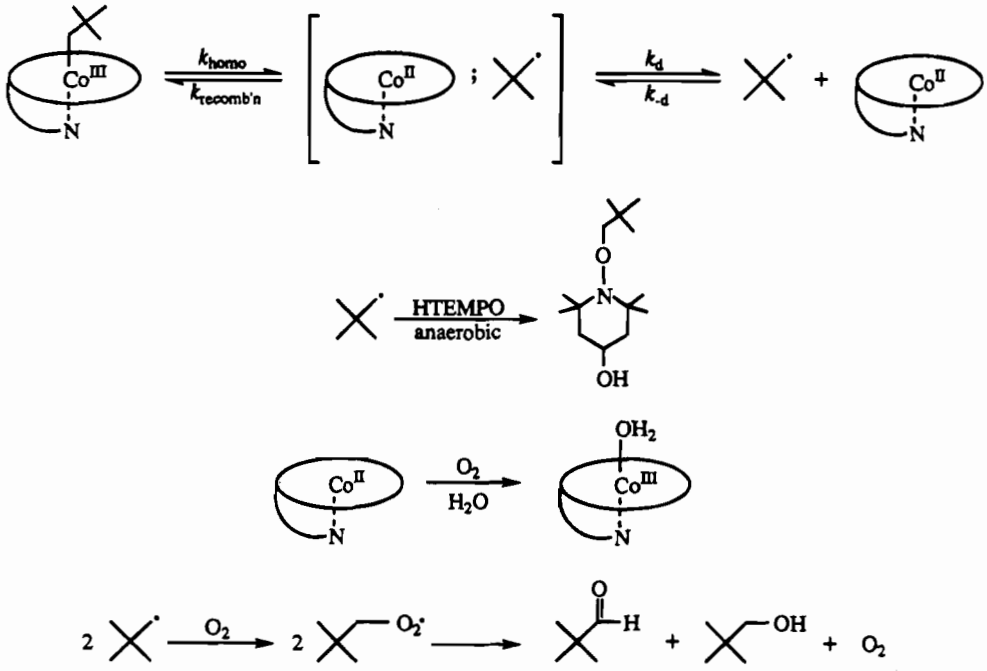

Table 1. Quantitative Analysis of the Products of Thermolysis of the *c* Side Chain Modified NpCbl Analogs

	yield (%)			
	NpCbl-*c*-COO^-	NpCbl-*c*-NHMe	NpCbl-*c*-NMe_2	NpCbl-*c*-NHiPr
Np-HTEMPO[a]	103 ± 6	86 ± 14	95 ± 4	96 ± 6
Co^{II} corrinoid[b]	106 ± 5	107 ± 4	89 ± 7	92 ± 3
Schiff base[c]	45 ± 8	47 ± 1	42 ± 6	44 ± 3

[a] Anaerobic decomposition at 50 °C in excess HTEMPO. Np-HTEMPO was quantitated by GC analysis using a standard curve obtained with authentic Np-HTEMPO. [b] Anaerobic decomposition at 30 °C in HTEMPO in Schlenk cuvettes. The cobalt(II) corrinoids were quantitated from their UV–visible spectra. [c] Aerobic decomposition at room temperature. The pivaladehyde formed was converted to its Schiff base with aniline (*N*-(2,2-dimethylpropylidene)benzeneamine) and quantitated by GC analysis using a standard curve obtained with the authentic Schiff base.

molysis reaction to completion.[3,13c,e,47,48] In the presence of oxygen, both of the homolysis products are trapped, as the cobalt(II) species is rapidly oxidized and the neopentyl radical undergoes a very rapid reaction with oxygen to form the neopentylperoxy radical.[49] The latter decomposes cleanly to pivalaldehyde and neopentanol.[10,13c,e]

Although it seems highly unlikely that alteration of the *c* side chain of NpCbl would alter the course of thermolysis, Scheme 1 was substantiated for the *c* side chain modified NpCbl analogs by quantitative determination of thermolysis products under anaerobic conditions in the presence of HTEMPO as well as in aerobic solution. In the presence of HTEMPO, anaerobic thermolysis led to essentially quantitative formation of the trapped organic radical, Np-HTEMPO, and to the appropriate *c* side chain modified cob(II)alamin analog, the latter being determined spectrophotometrically (Table 1). For thermolyses in aerobic solution, the pivalaldehyde product was assayed by GC after conversion to its Schiff base with aniline. The results (Table 1) are consistent with the expected 50% yield of aldehyde based on stoichiometry (Scheme 1). These product determinations adequately demonstrate that the course of the thermolysis reaction of NpCbl remains the same when the *c* side chain is modified by amide hydrolysis or by N-alkylation.

Thermolysis Kinetics. Aerobic thermolysis of the *c* side chain modified NpCbl analogs at pH 7.5 proceeded with clean spectral changes displaying multiple isosbestic points (e.g., 251, 270, 281, 334, 369, and 470 nm for NpCbl-*c*-COO^- at 25 °C). Single wavelength absorbance changes at the γ band maximum for the H_2OCbl analog product (at or near 350 nm) were first order and were fitted to an exponential function using a nonlinear least squares algorithm. The weighted average of four or five rate constant determinations at each temperature was taken as the best estimate of the rate constant, k_{neut}, for thermolysis of the neutral species of each analog. These values are accumulated in Table 2. As a further check on the applicability of Scheme 1 and the assumption that oxygen trapping of radicals under aerobic conditions is sufficiently rapid, rate constants for thermolysis of each of the NpCbl analogs were measured under anaerobic conditions at 30.0 °C in the presence of 1.0×10^{-3} M HTEMPO. As seen in Table 2, these rate constants are in very good agreement with those obtained from aerobic thermolysis at 30.0 °C.

These rate constants do not reflect the thermolysis of the base-on species of these NpCbl analogs since, as discussed below, significant amounts of the base-off (but Bzm unprotonated) species exist under these conditions. Nonetheless, Eyring plots (representative data are shown in Figure 2) were linear, giving rise to the observed activation parameters, $\Delta H^{\ddagger}_{obs}$ and $\Delta S^{\ddagger}_{obs}$, listed in Table 3. For these analyses, the observed uncertainties in k_{neut} and T were propagated through the Eyring equation as

(47) (a) Daikh, B. E.; Hutchison, J. E.; Gray, N. E.; Smith, B. L.; Weakley, T. J. R.; Finke, R. G. *J. Am. Chem. Soc.* **1990**, *112*, 7830. (b) Daikh, B. E.; Finke, R. G. *J. Am. Chem. Soc.* **1991**, *113*, 4160.

(48) (a) Finke, R. G.; Smith, B. L.; Mayer, B. J.; Molinero, A. A. *Inorg. Chem.* **1983**, *22*, 3677. (b) Hay, B. P.; Finke, R. G. *Polyhedron* **1988**, *7*, 1469. (c) Martin, B. D.; Finke, R. G. *J. Am. Chem. Soc.* **1990**, *112*, 2419. (d) Martin, B. D.; Finke, R. G. *J. Am. Chem. Soc.* **1992**, *114*, 585. (e) Garr, C. D.; Finke, R. G. *J. Am. Chem. Soc.* **1992**, *114*, 10440.

(49) $k_2 = 2.65 \times 10^9$ $M^{-1}s^{-1}$. Marchaj, A.; Kelley, D. G.; Bakac, A.; Espenson, J. H. *J. Phys. Chem.* **1991**, *95*, 4440.

Table 2. Averaged Rate Constants, k_{neut}, for the Aerobic Thermolysis of the *c* Side Chain Modified NpCbl Analogs in Neutral Aqueous Solution[a]

NpCbl-*c*-COO$^-$		NpCbl-*c*-NHMe		NpCbl-*c*-NMe$_2$		NpCbl-*c*-NHiPr	
T, °C	k_{neut}, s^{-1}	*T*, °C	k_{neut}, s^{-1}	*T*, °C	k_{neut}, s^{-1}	*T*, °C	k_{neut}, s^{-1}
15.0	$(1.74 \pm 0.28) \times 10^{-5}$	10.1	$(1.28 \pm 0.09) \times 10^{-5}$	9.8	$(1.73 \pm 0.12) \times 10^{-5}$	10.1	$(1.01 \pm 0.01) \times 10^{-5}$
20.0	$(4.19 \pm 0.06) \times 10^{-5}$	14.9	$(2.93 \pm 0.10) \times 10^{-5}$	15.1	$(4.28 \pm 0.09) \times 10^{-5}$	16.0	$(2.70 \pm 0.10) \times 10^{-5}$
25.1	$(9.37 \pm 0.14) \times 10^{-5}$	20.0	$(6.87 \pm 0.19) \times 10^{-5}$	20.0	$(9.41 \pm 0.12) \times 10^{-5}$	20.0	$(5.15 \pm 0.09) \times 10^{-5}$
29.9	$(2.02 \pm 0.01) \times 10^{-4}$	25.0	$(1.49 \pm 0.04) \times 10^{-4}$	25.0	$(2.12 \pm 0.01) \times 10^{-4}$	25.1	$(1.11 \pm 0.01) \times 10^{-4}$
30.0	$(1.88 \pm 0.02) \times 10^{-4}$ [b]	30.0	$(3.31 \pm 0.01) \times 10^{-4}$	30.0	$(4.65 \pm 0.04) \times 10^{-4}$	30.1	$(2.53 \pm 0.02) \times 10^{-4}$
34.9	$(4.16 \pm 0.04) \times 10^{-4}$	30.0	$(3.69 \pm 0.03) \times 10^{-4}$ [b]	30.0	$(4.59 \pm 0.35) \times 10^{-4}$ [b]	30.0	$(2.32 \pm 0.21) \times 10^{-4}$ [b]
40.0	$(8.33 \pm 0.31) \times 10^{-4}$	35.1	$(6.80 \pm 0.02) \times 10^{-4}$	35.0	$(9.60 \pm 0.05) \times 10^{-4}$	35.0	$(5.09 \pm 0.04) \times 10^{-4}$
45.0	$(1.57 \pm 0.14) \times 10^{-3}$	40.0	$(1.34 \pm 0.01) \times 10^{-3}$	40.0	$(1.81 \pm 0.03) \times 10^{-3}$	40.0	$(1.04 \pm 0.01) \times 10^{-3}$
49.9	$(2.70 \pm 0.02) \times 10^{-3}$						

[a] In potassium phosphate buffer, pH 7.5, ionic strength 1.0 M (KCl). Each rate constant is the weighted average of four or five determinations. [b] Single determination under anaerobic conditions in the presence of 1×10^{-3} M HTEMPO.

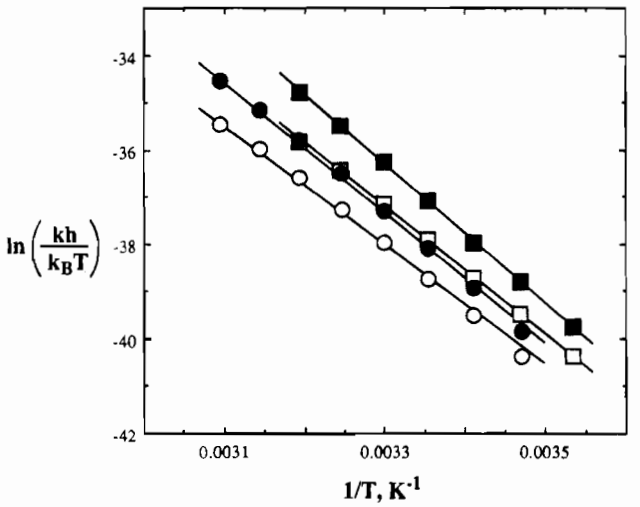

Figure 2. Representative Eyring plots of the observed (k_{neut}) rate constatns for thermolysis of the neutral species of NpCbl-*c*-COO$^-$ (○) and NpCbl-*c*-NMe$_2$ (□) and of the corrected rate constants (k_{on}) for thermolysis of the base-on species of NpCbl-*c*-COO$^-$ (●) and NpCbl-*c*-NMe$_2$ (■). The solid lines are weighted least squares regression lines: k_{neut}, NpCbl-*c*-COO$^-$, slope = $-1.259 \pm 0.004 \times 10^4$ K, intercept = 3.54 ± 0.12, $r^2 = 0.9990$, k_{neut}, NpCbl-*c*-NMe$_2$, slope = $-1.355 \pm 0.005 \times 10^4$ K, intercept = 7.52 ± 0.18, $r^2 = 0.9997$, k_{on}, NpCbl-*c*-COO$^-$, slope = $-1.382 \pm 0.007 \times 10^4$ K, intercept = 8.26 ± 0.22, $r^2 = 0.9990$, k_{on}, NpCbl-*c*-NMe$_2$, slope = $-1.476 \pm 0.011 \times 10^4$ K, intercept = 12.42 ± 0.35, $r^2 = 0.9998$.

previously described[13d] and the data fit to a straight line via a weighted least-squares procedure to provide the best estimates of the activation parameters and their errors.

Axial Nucleotide Coordination Equilibria. Even in neutral solution, where the axial Bzm nucleotide is completely deprotonated, it is clear that NpCbl,[8,13a,d,14] as well as Np-8-epiCbl and Np-13-epiCbl,[13e] exists significantly as the base-off species. For these compounds, the base-off species is at least 2 orders of magnitude less thermally reactive than the base-on species.[13a,e,14] Consequently, the rate constant for thermolysis of the base-on species, k_{on}, can be calculated from the rate constant for thermolysis of the neutral species, k_{neut}, as $k_{on} = k_{neut}/f_{on}$, where f_{on} is the fraction of the NpCbl analog present as the base-on species at neutral pH. In order to make such calculations, accurate values for the equilibrium constant, K_{meas},[50] for the base-off/base-on equilibrium are needed.

Previous work[13d,e,14,50] has shown that an NMR method can be successfully used to evaluate the enthalpy, ΔH_{meas}, and entropy, ΔS_{meas}, changes associated with the off/on equilibrium, thus permitting calculation of the equilibrium constant at any temperature. This method originally utilized the ^{13}C NMR chemical shifts of RCbls enriched in ^{13}C in the α carbon of the organic ligand. Since the enthalpy of formation of the base-on species of RCbls is negative,[20,50,51] as the temperature is increased, the base-off species is favored, and the ^{13}C NMR resonance frequency of, for instance, $^{13}CH_3$Cbl shifts toward the value of its base-off analog, $^{13}CH_3$Cbi$^+$.[50] Thus, the temperature dependence of the difference in resonance frequency between the RCbl and its RCbi$^+$ base-off analog can be used to determine the enthalpy and entropy of the base-off/on equilibrium.[52] Waddington and Finke[14] greatly extended the range of this method by use of the C10H ^{1}H resonance of NpCbl, which was shown to be sufficiently sensitive to the off/on transition to provide a precise measure of the position of this equilibrium. This method has now been successfully applied to NpCbl in CD_3OD[14] and in D_2O,[13d] and to Np-13-epiCbl in D_2O.[13e]

We have consequently used the C10H ^{1}H NMR method to determine the thermodynamic parameters for the base-off/on equilibrium of the *c* side chain modified NpCbl analogs. Representative data are shown in Figure 3, and the values of ΔH_{meas} and ΔS_{meas}, as well as calculated values of K_{meas} and f_{on} at 25.0 °C for these compounds and for NpCbl itself are given in Table 3. In order to determine if the rate constants for thermolysis of the base-off species are indeed negligible compared to those of the base-on species, the rate of thermolysis of the protonated base-off species of each NpCbl derivative (in 0.5 M HCl) was monitored at a single temperature (35.0 °C) by scanning the UV−visible spectrum periodically over a period of several days. As the reactions were too slow to follow to completion, the samples were photolyzed to provide an approximate final spectrum and allow an estimation of the rate constant. In each case, the thermolysis of the base-off species was at least 2 orders of magnitude slower than that of the neutral species, and approximately 3 orders of magnitude slower than the base-on species.[53] Corrected values for the rate constants for thermolysis of the base-on species, k_{on}, of these NpCbl

(50) Brown, K. L.; Peck-Siler, S. *Inorg. Chem.* **1988**, *27*, 3548.

(51) Brown, K. L.; Wu, G.-Z. *Inorg. Chem.* **1994**, *33*, 4122.

(52) The equation describing the dependence of $\Delta\nu_{obs}$, the difference in resonance frequency between the RCbl and its RCbi$^+$ base-off analog is

$$\nu_{obs} = \{\Delta\nu_o \exp[(\Delta S_{meas}/R) - (\Delta H_{meas}/RT)]\}/\{1 + \exp[(\Delta S_{meas}/R) - (\Delta H_{meas}/RT)]\}$$

where $\Delta\nu_o$ is the difference in resonance frequency at 0 K, and ΔH_{meas} and ΔS_{meas} are the enthalpy and entropy changes, respectively, associated with the equilibrium constant, K_{meas},[50] for the conversion of all base-off species to the base-on species.

(53) For example, the rate constant for thermolysis of base-off NpCbl-*c*-COO$^-$ at 35 °C was approximately 5.0×10^{-7} s^{-1}, making it 840-fold slower than the neutral species and 1800-fold slower than the base-on species.

Table 3. Activation Parameters for Thermolysis and Thermodynamic Parameters for the Base-off/Base-on Equilibrium of NpCbl and its *c* Side Chain Modified Analogs

	NpCbl-*c*-COO$^-$	NpCbl[a]	NpCbl-*c*-NHMe	NpCbl-*c*-NMe$_2$	NpCbl-*c*-NHiPr
$\Delta H^{\ddagger}_{obs}$,[b] kcal mol^{-1}	25.0 ± 0.1	26.5 ± 0.1	26.1 ± 0.1	26.9 ± 0.1	26.8 ± 0.1
$\Delta S^{\ddagger}_{obs}$,[b] cal mol^{-1} K^{-1}	7.0 ± 0.2	12.5 ± 0.3	11.5 ± 0.4	14.9 ± 0.4	13.5 ± 0.3
ΔH_{meas},[c] kcal mol^{-1}	−3.9 ± 0.3	−4.1 ± 0.1	−5.1 ± 0.3	−4.6 ± 0.3	−2.6 ± 0.3
ΔS_{meas},[c] cal mol^{-1} K^{-1}	−12.9 ± 0.6	−12.5 ± 0.3	−16.2 ± 0.7	−16.0 ± 0.6	−12.4 ± 0.6
$\Delta H^{\ddagger}_{on}$,[d] kcal mol^{-1}	27.5 ± 0.1	28.3 ± 0.2	28.7 ± 0.2	29.4 ± 0.2	29.1 ± 0.1
$\Delta S^{\ddagger}_{on}$,[d] cal mol^{-1} K^{-1}	16.4 ± 0.4	19.3 ± 0.6	21.1 ± 0.7	24.8 ± 0.6	24.9 ± 0.3
K_{meas}[e]	1.13	1.73	1.61	0.78	0.16
f_{on}[f]	0.53	0.63	0.62	0.44	0.14
k_{on}, s^{-1}	1.80 × 10^{-4}	1.96 × 10^{-4}	2.45 × 10^{-4}	4.80 × 10^{-4}	8.38 × 10^{-4}

[a] Reference 13d. [b] Observed activation parameters for thermolysis of the neutral species. [c] Thermodynamic parameters for the base-off/on equilibrium. [d] Activation parameters for the base-on species. [e] Equilibrium constant for the base-off/on equilibrium at 25.0 °C. [f] Calculated fraction of the NpCbl analog as the base-on species at 25.0 °C. [g] Calculated value for the thermolysis rate constant for the base-on species at 25.0 °C.

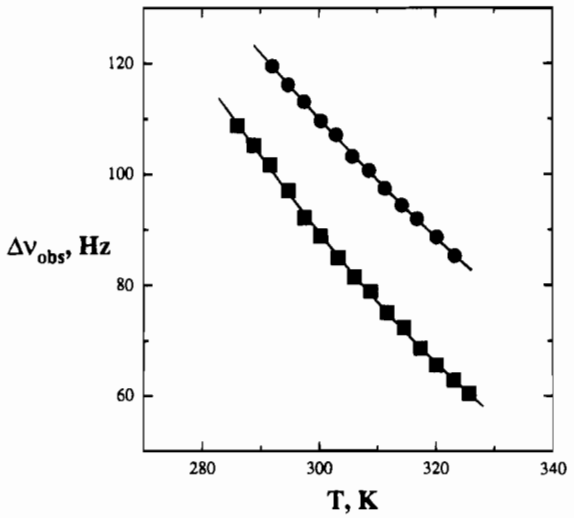

Figure 3. Plots of $\Delta\nu_{obs}$, the absolute magnitude of the difference in ^{1}H NMR resonance frequency between the C10 hydrogen of NpCbl-*c*-COO$^-$ and NpCbi-*c*-COO (●) or of NpCbl-*c*-NMe$_2$ and NpCbi-*c*-NMe$_2^+$ (■). The solid lines are nonlinear least squares regressions (see ref 52) from which the values $\Delta H_{meas} = -3.91 \pm 0.26$ kcal mol^{-1}, $\Delta S_{meas} = -12.9 \pm 0.6$ cal mol^{-1} K^{-1}, and $\Delta\nu_o = 211.3 \pm 1.5$ Hz were obtained for NpCbl-*c*-COO$^-$ and $\Delta H_{meas} = -4.64 \pm 0.26$ kcal mol^{-1}, $\Delta S_{meas} = -16.0 \pm 0.6$ cal mol^{-1} K^{-1}, and $\Delta\nu_o = 208.1 \pm 1.7$ Hz were obtained for NpCbl-*c*-NMe$_2$.

analogs were consequently calculated as above, and used to determine the activation parameters, $\Delta H^{\ddagger}_{on}$ and $\Delta S^{\ddagger}_{on}$, for the base-on species from Eyring plots (see Figure 2 for representative data). The resulting activation parameters are given in Table 3, along with calculated values of k_{on} at 25 °C. As can be seen in Table 3, the values of $\Delta H^{\ddagger}_{on}$ vary little across the series of five compounds, the weighted average value being 28.4 ± 1.1 kcal mol^{-1}. However, the values of $\Delta S^{\ddagger}_{on}$ increase in the order NpCbl-*c*-COO$^-$, NpCbl, NpCbl-*c*-NHMe, NpCbl-*c*-NMe$_2$, and NpCbl-*c*-NHiPr from 16.4 ± 0.4 to 24.9 ± 0.3 cal mol^{-1} K^{-1}, although the last two derivatives have essentially the same value.

Molecular Mechanics Calculations. In order to explore the effects of *c* side chain modification on the freedom of rotation of this side chain, molecular mechanics (MM) calculations were carried out using the force field recently developed[37] specifically for cobalamins. The effects of *c* side chain substitution were studied by determining the effect of rotation about the C7−C37 bond by driving the C6−C7−C37−C38 torsional angle, ω_1, through 360° in steps of 10°. The Co−C bond length, and the Co−C−C and Co−C−H bond angles at each value of ω_1 were extracted from the output files of the energy-minimized structure. Direct comparison of the strain energies of different molecules is impossible since the total strain energy depends on the number of atoms in each molecule. Consequently,

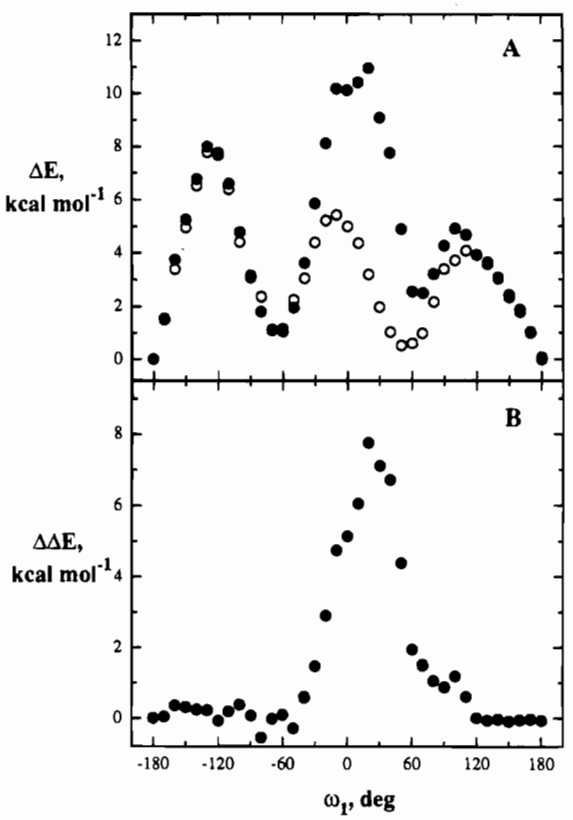

Figure 4. (A) Plot of the relative strain energy, ΔE, for NpCbl-*c*-NHiPr (●) and for CH_3Cbl-*c*-NHiPr (○) vs ω_1, the C6−C7−C37−C38 torsion angle, as the *c* side chain is rotated about the C7−C37 bond. The relative strain energy is defined as the difference between the absolute strain energy at a given value of ω_1, and the minimum absolute strain energy (i.e., when $\omega_1 = \pm 180°$). (B) Plot of the difference in relative strain energy, $\Delta\Delta E$, between NpCbl-*c*-NHiPr and CH_3Cbl-*c*-NHiPr as a function of ω_1, the C6−C7−C37−C38 torsion angle, as the *c* side chain is rotated about the C7−C37 bond.

relative strain energies, ΔE, were defined as the difference between the strain energy at each ω_1, and the minimum strain energy (always observed at $\omega_1 = \pm 180°$). Values of ΔE were plotted vs ω_1, and the integrated strain energy, E_{str}, was determined numerically by integratng the area under the curve. An example is shown in Figure 4A for NpCbl-*c*-NHiPr.

The strain energy profiles were similar for each of the five complexes. Three maxima and three minima were evident in each profile. The global minimum always occurred at $\omega_1 = \pm 180°$ when C37 is vertically above C7 and the *c* side chain is pointing outward from the molecule. A view down the C37−C7 bond (from the upper corrin face) finds the C36 methyl and the *c* side chain C37 methylene in an approximately gauche arrangement with the C36−C7−C37−C38 torsion angle at

Table 4. Molecular Mechanics Results for the *c* Side Chain Modified NpCbl and CH_3Cbl Analogs

c side chain	R	E_{str},[a] kcal deg mol^{-1}	ΔE_{str},[b] kcal deg mol^{-1}	Co−C,[c] Å	Co−C−C,[d] deg	Co−C−H,[e] deg	van der Waals vol, $Å^3$
$-COO^-$	Np	1249	365	2.068 ± 0.005	131.9 ± 0.2	101.2 ± 1.4, 103.3 ± 1.1	48.5
	CH_3	884		1.985 ± 0.002		112.6 ± 0.1, 109.6 ± 0.6, 112.9 ± 0.7	
$-CONH_2$	Np	1416	398	2.068 ± 0.006	132.0 ± 0.3	101.1 ± 1.7, 103.3 ± 1.4	58.2
	CH_3	1018		1.985 ± 0.002		112.6 ± 0.2, 109.8 ± 0.7, 112.7 ± 0.8	
−CONHMe	Np	1569	407	2.069 ± 0.006	132.4 ± 0.4	101.0 ± 1.5, 102.6 ± 1.5	82.7
	CH_3	1162		1.985 ± 0.002		112.8 ± 0.8, 109.8 ± 0.7, 112.7 ± 0.8	
$-CONMe_2$	Np	1628	459	2.069 ± 0.007	132.0 ± 0.3	100.8 ± 1.8, 103.2 ± 1.5	106.2
	CH_3	1169		1.984 ± 0.003		112.8 ± 0.6, 109.6 ± 1.1, 112.8 ± 1.0	
−CONHiPr	Np	1722	546	2.068 ± 0.007	131.9 ± 0.2	101.1 ± 1.5, 103.4 ± 1.3	130.4
	CH_3	1176		1.984 ± 0.004		113.1 ± 0.9, 109.4 ± 1.0, 112.6 ± 0.5	

[a] Integrated strain energy, calculated as the area under the plot of ΔE, the strain energy relative to the minimum value, vs ω_1, the C6−C7−C37−C38 torsion angle. [b] Difference in integrated strain energy, E_{str}, for the NpCbl analog and the corresponding CH_3Cbl analog. [c] Average Co−C bond length (± one standerd deviation) for the 36 rotational positions of the *c* side chain. The weighted average of the average Co−C bond distance for all 5 NpCbl analogs is 2.068 ± 0.002 Å (99% confidence interval). [d] Average Co−C−C bond angle (± one standard deviation) for the 36 rotational positions of the *c* side chain. The weighted average for all 5 NpCbl analogs is 132.0 ± 0.5° (99% confidence interval). [e] Average Co−C−H bond angles (± one standard deviation) for the 36 rotational positions of the *c* side chain. The weighted averages for all 5 NpCbl analogs are 101.1 ± 0.6° and 103.3 ± 1.4° (99% confidence intervals).

−56°. Rotation of the *c* side chain in a counterclockwise direction, as seen from the β ("upper") face of the molecule, brings the *c* side chain over C36. The energy barrier at about −100° is principally due to close contact between the *c* side chain, particularly the carbonyl oxygen, O39, and the C36 hydrogen atoms. Continued rotation in this direction brings the side chain over the C5 region of the molecule (the energy minimum at −80°), and then, as ω_1 continues to increase toward 0, a close contact occurs between the *c* side chain and the coordinated Np ligand. As the *c* side chain rotates past the coordinated Np, the strain energy decreases and the minimum near 60° finds the side chain over the C10 hydrogen atom. The energy barrier at around 100° occurs as the side chain passes over the vertically projecting hydrogen at C8.

In order to try to isolate the relative barrier to *c* side chain rotation due to close contact with the Np ligand and factor out the barriers to rotation due to the C36 methyl and the C8 hydrogen, we also studied the effect of *c* side chain rotation in CH_3Cbl and its *c* side chain modified analogs. A strain energy profile for CH_3Cbl-*c*-NHiPr is shown as an example in Figure 4A. Three barriers to rotation are again found, but the central one, due to contact with the alkyl ligand, is much reduced as anticipated. Subtraction of the relative strain energies for the CH_3 derivative from those for the Np derivative, $\Delta\Delta E = \Delta E_{Np} - \Delta E_{CH_3}$, results in the profile shown in Figure 4B, in which the barriers to rotation due to the C36 methyl and C8 hydrogen are substantially canceled. Consequently, the differential integrated strain energy, ΔE_{str}, was calculated as the difference between the integrated strain energies of the NpCbl derivative and that of its CH_3Cbl partner, $\Delta E_{str} = E_{str}^{Np} - E_{str}^{CH_3}$, and represents the additional strain imposed by the larger ligand in the β coordination site.

Values for the integrated strain energies for the neopentyl and methyl derivatives of Cbl and each *c* side chain modified analog are given in Table 4, along with the differential integrated strain energies, the average Co−C bond lengths, and the average Co−C−C and Co−C−H bond angles. Both the integrated strain energies and the differential integrated strain energies for the NpCbl analogs increase monotonically as the *c* side chain substituent, X (Figure 1), is varied through the series X = O^-, NH_2, NHMe, NMe_2, and NHiPr. Most importantly, the Co−C bond lengths, and Co−C−C and Co−C−H bond angles for the NpCbl derivatives are essentially invariant as the *c* side chain is rotated through 360° about the C7−C37 bond. Similarly, the Co−C bond length and the Co−C−C and Co−C−H bond angles do not vary significantly across the series of compounds, the weighted average values being 2.068 ± 0.002 Å, 132.0 ± 0.5°, and 101.1 ± 0.6° and 103.3 ± 1.4°, respectively, the stated uncertainties being 99% confidence intervals. These results strongly suggest that increasing bulk of the *c* side chain substituent does not stretch or distort the Co−C bond so that ground state enthalpic destabilization of NpCbl toward Co−C bond homolysis is not occurring in these analogs. These MM results are in agreement with the observation that the enthalpies of activation for thermolysis of the base-on species (Table 3) vary very little across the series of NpCbl analogs.

The average Co−C bond length (2.068 ± 0.002 Å) and Co−C−C bond angle (132.0 ± 0.5°) calculated for the NpCbl series are both quite large, but nonetheless compare very favorably to the observed values for neopentyl(pyridine)cobaloxime (2.060 ± 0.006 Å and 130.3 ± 0.4°, respectively).[54] Similarly, the average calculated value for the Co−C bond length of the series of CH_3Cbl analogs (1.985 ± 0.002 Å) is in excellent agreement with the X-ray crystal structure value for CH_3Cbl itself (1.99 Å).[55] These observations inspire substantial confidence in the force field developed for these MM calculations.[37]

In order to attempt to determine the steric bulk of the *c* side chain substituents, −COX (Figure 1), the van der Waals volumes of these groups were estimated as described in the Experimental Section. The values obtained are listed in Table 4 which shows that the van der Waals volumes increase in the order X = O^-, NH_2, NHMe, NMe_2, and NHiPr, from about 50 to 130 $Å^3$. There is thus a clear relationship between the size of the *c* side chain substituent and the strain energy generated by rotation of this side chain, regardless of whether the latter is expressed as the integrated strain energy of the NpCbl analogs or the difference in integrated strain energies between the NpCbl analogs and the corresponding CH_3Cbls. Importantly, there is also a relationship between the entropy of activation for thermal Co−C bond homolysis of the base-on species of a NpCbl analog and the strain energy generated by *c* side chain rotation, as shown in Figure 5. Thus, the entropy of activation increases monotonically with the differential integrated strain energy, ΔE_{str}, but shows a distinct tendency to level off at ≈ 25 cal mol^{-1} K^{-1} as the strain energy exceeded ≈ 450 kcal deg mol^{-1}.

Finally, in order to determine the influence of Co−C bond homolysis on the steric barrier to *c* side chain rotation, the differential integrated strain energies for this rotation were calculated for various separations between the Np• radical and

(54) Randaccio, L.; Bresciani-Pahor, N.; Toscana, P. J.; Marzilli, L. G. *J. Am. Chem. Soc.* **1981**, *103*, 6347.
(55) Rossi, M.; Glusker, J.; Randaccio, L.; Summers, M. F.; Toscano, P. J.; Marzilli, L. G. *J. Am. Chem. Soc.* **1985**, *107*, 1729.

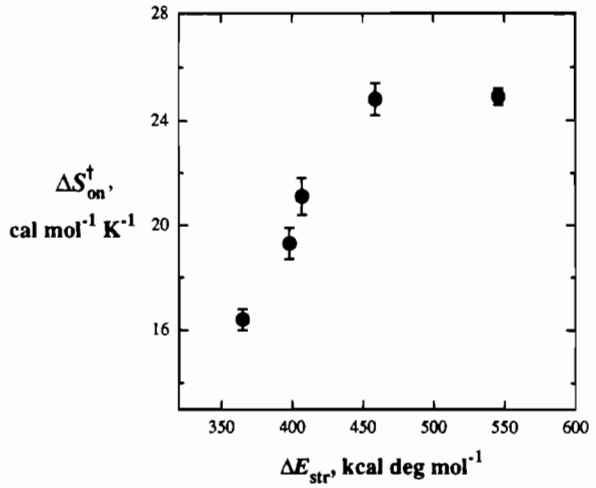

Figure 5. Plot of the entropy of activation, $\Delta S^{\ddagger}_{on}$, for thermolysis of the base-on species of NpCbl and its *c* side chain modified analogs vs the differential integrated strain energy, ΔE_{str}, due to rotation of the *c* side chain about the C7−C37 bond.

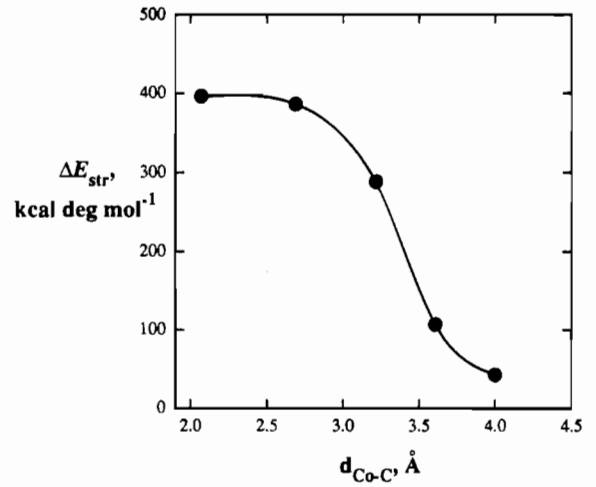

Figure 6. Plot of the differential integrated strain energy, ΔE_{str}, for *c* side chain rotation in NpCbl vs the Co−C internuclear separation.

the Co^{II} complex by varying the equilibrium strain-free Co−C bond length. The results (Figure 6) show that the steric contact between the *c* side chain and the Np ligand decreases rapidly as the Co−C bond is stretched past ~3 Å.

Discussion

Synthesis of CNCbl-*c*-COO^- by reduction of the *c*-lactone provides ready access to *c* side chain modified cobalamins. There are no reports in the literature of the preparation of CNCbl-*a*- or -*g*-monocarboxylate, and our efforts to prepare these important derivatives have been unsuccessful. The dim prospects for obtaining the monocarboxylates of the other two upward projecting acetamide side chains make an understanding of the extent to which *c* side chain thermal motions can contribute to the entropic activation of RCbls for C−Co bond homolysis that much more compelling.

The activation parameters for thermolysis of the *c* side chain modified NpCbl-*c*-COX compounds (Table 3) and the molecular mechanics analysis of the consequences of rotation of the *c* side chain about the C7−C37 bond (Table 4) argue strongly that substitution at the *c* side chain, even with very bulky groups, does not enthalpically activate these complexes for Co−C bond homolysis. Neither complete rotation of the *c* side chain about the C7−C37 bond nor substitution at the *c* carbonyl with increasingly bulky groups has any significant effect on the Co−C bond length or any of the Co−C−C or Co−C−H bond angles. Thus, no strain appears to develop in the Co−C bond as a result of steric interactions between the *c* carbonyl substituent and the organic ligand. As a consequence, there is little variation in the enthalpy of activation of the NpCbl-*c*-COX complexes with the bulk of X, the weighted average, 28.4 ± 1.1 kcal mol^{-1}, encompassing all of the observed values within ±1 standard deviation. We conclude that the effect of the steric bulk of the *c* carbonyl substituent on the rate of thermolysis is essentially an entropic effect, a conclusion born out by the increase in the entropy of activation for thermolysis by 8.5 ± 0.6 cal mol^{-1} K^{-1} as the steric bulk of the *c*-COX substituent is increased from $-COO^-$ to $-CONMe_2$ or −CONHiPr.

As the thermal homolysis of RCbls is well-known to proceed via a caged radical pair,[14,42−44] the possibility that the increase in the observed entropy of activation for the NpCbl-*c*-COX complexes with increasing bulk of X is due to the influence of these structural changes on the cage effect,[56] must be examined. For the general scheme for metal−ligand bond dissociation of Koenig and Finke[56] (eq 1), the observed entropy of activation

$$M{-}L \underset{k_c}{\overset{k_1}{\rightleftharpoons}} \overline{[M^{\bullet}\ L^{\bullet}]} \underset{k_{-1}}{\overset{k_d}{\rightleftharpoons}} M^{\bullet} + L^{\bullet} \qquad (1)$$

is given by eq 2,[57] where the fractional cage efficiency, F_c, is

$$\Delta S^{\ddagger}_{obs} = \Delta S_{\ddagger 1} + F_c[\Delta S^{\ddagger}_{d} - \Delta S^{\ddagger}_{c}] \qquad (2)$$

given by eq 3. The term $[\Delta S^{\ddagger}_{d} - \Delta S^{\ddagger}_{c}]$ is expected to be

$$F_c = k_c/(k_c + k_d) \qquad (3)$$

positive[56] since $\Delta S^{\ddagger}_{d}$ is the entropy of activation for diffusive separation of the caged pair, while $\Delta S^{\ddagger}_{c}$ is the entropy of activation for in-cage recombination. This term is not expected to be significantly affected by the structural modifications in the NpCbl-*c*-COX series. However, the fractional cage efficiency could be affected by these alterations in structure. While the diffusion rate constant, k_d, should be relatively unaffected by these structural modification since the shape of the NpCbl-*c*-COX complexes is constant and the mass varies by only 3.2% across the series, the in-cage recombination rate, k_c, could be affected by the changes in steric bulk of the *c* side chain. However, if increases in the steric bulk of the *c* side chain do significantly affect k_c, they must surely do so by sterically hindering the recombination reaction. Thus, F_c is expected to decrease with increasing bulk of the substituent, X. Consequently, differential cage effects seem unlikely to provide an explanation for the increase in the observed entropy of activation with increasing steric bulk of the c side chain and suggest that the increase in Co−C bond homolysis activation entropy is, if anything, underestimated because of such cage effects.

The molecular mechanics results (Table 4) suggest that this entropic effect is the result of increasing restriction of the freedom of motion of the *c* side chain due to steric interactions between the Np ligand and the increasingly bulky *c* side chain substituent. Thus, as the van der Waals volume of the *c*-COX moiety increases by more than 2-fold, the integrated strain energy due to rotation of the *c* side chain about the C7−C37 bond increases as does the height of the energy barrier to rotation

(56) (a) Koenig, T.; Finke, R. G. *J. Am. Chem. Soc.* **1988**, *110*, 2657. (b) Koenig, T. W.; Hay, B. P.; Finke, R. G. *Polyhedron* **1988**, *7*, 1499.

(57) Koenig and Finke[56] have pointed out that eq 2 is an approximation in the range $0.1 < F_c < 0.9$, but is accurate outside this range. Garr and Finke[48e] have determined $F_c \geq 0.94$ for the [Ado•; cob(II)inamide] radical pair in ethylene glycol at ~110 °C.

past the Np ligand. It is difficult to avoid the conclusion that as the *c*-COX moiety becomes larger, fewer and fewer *c* side chain conformations about the C7−C37 bond can be adopted due to close contact with the Np ligand, leading to a decrease in the ground state entropy of the complex.

The data in Figure 6 show that the steric barrier to *c* side chain rotation due to the Np ligand does, indeed, decrease significantly as the Co−C bond is lengthened. While the internuclear distance in the homolysis transition state for NpCbl is unknown, *ab initio* calculations of the transition state geometries for C−H and O−H bond homolysis in the methoxy and hydroxymethyl radicals[58] show that the ratio of the transition state internuclear distance to the ground state equilibrium distance is about 1.6. If this figure is approximately correct for the Co−C bond homolysis of NpCbl, the differential integrated strain energy for *c* side chain rotation would be reduced by about 2-fold in the transition state ($d_{Co-C} \sim 3.3$ Å), from nearly 400 to about 200 kcal deg mol^{-1}. This is larger than the proportional decrease in going from NpCbl-*c*-NHiPr to NpCbl-*c*-COO$^-$ (Table 4) and would consequently be expected to significantly affect the side chain rotational entropy.

As seen in Figure 5, there is, as might be expected, a limit to the amount of entropic destabilization which can be obtained from restriction of *c* side chain mobility. Thus, as the van der Waals volume of the COX moiety exceeds 100 Å^3 and the *c* side chain differential rotational strain energy exceeds about 450 kcal deg mol^{-1}, the entropy of activation for thermolysis of the base-on species levels off at about 25 cal mol^{-1} K^{-1}, a value some 5.6 ± 0.6 cal mol^{-1} K^{-1} larger than that for NpCbl itself. It seems reasonable to conclude that once the *c*-COX moiety has reached this size, the *c* side chain is effectively excluded from adopting any conformations in which the C37−C38 bond points toward the "interior" of the molecule and that further increases in steric bulk will have little or no additional effect on *c* side chain mobility. We conclude that approximately 5.6 cal mol^{-1} K^{-1} is the maximal entropic destabilization of NpCbl for thermal homolysis that can be obtained by ground state restriction of the mobility of the *c* side chain.

The situation regarding the thermal mobility of Cbl side chains could be considerably different in an enzyme active site than in solution. In solution, when the *c* side chain is restricted from adopting any "inwardly" projecting conformations due to the bulk of its substituent, it may still adopt many "outwardly" projecting conformations. This is why only a portion of the net rotational entropy of the side chain is available for ground state destabilization under these conditions. This may not be the case in a protein binding pocket where nearby amino acid residues may sterically prevent the rotation of side chains out and away from the coenzyme interior. Thus, in the enzyme-bound ground state, there may be little freedom for the corrin ring side chains to rotate "outwardly", and little freedom to rotate "inwardly" due to the bulky organic ligand. In the homolysis transition state, new side chain conformations utilizing the "interior" space would presumably become available due to the incipient departure of the Ado· radical, as suggested by the results in Figure 6. This would provide an entropic driving force for Co−C bond cleavage resulting in entropic catalysis of AdoCbl homolysis.

The value of 5.6 ± 0.6 cal mol^{-1} K^{-1} for the maximum entropic destabilization of NpCbl by *c* side chain rotational restriction can be used to estimate the amount of entropic destabilization of AdoCbl which might be obtained in the enzymatic activation of AdoCbl if these enzymes utilize such a mechanism. If the entropic effect of restricting side chain mobility is approximately the same for all 3 upward projecting acetamide side chains, ~17 cal mol^{-1} K^{-1} of entropic driving force could be generated by such a mechanism. This would represent about 30% of the decrease in the free energy of activation for AdoCbl homolysis brought about by the enzyme ethanolamine deaminase at 25 °C or about 39% for the AdoCbl-dependent ribonucleotide reductase.[15]

Such an estimate requires some assumptions. First, rotation of the *a* and *g* side chains are assumed to be able to make the same contribution to the entropy of activation as the *c* side chain. While the *a* and *g* side chains are actually closer to the Ado ligand in the X-ray crystal structures of AdoCbl,[59,60] the structures of the three side chains are identical, suggesting that the entropic consequences of their internal rotations should be expected to be the same.

Second, is the possibility that steric interactions between upward projecting acetamide side chains and bulky β axial ligands engender a downward flexing of the corrin ring. Such an effect is thought to be responsible for the low binding constants for the Bzm moiety to the cobalt atom in RCbls with bulky primary or secondary alkyl ligands.[8,13a,61] This effect is apparently transmitted via close contacts between the downward projecting *b*, *d*, and *e* propionamide side chains and the axial Bzm.[37,51] Indeed, the failure to observe any distortions of the Co−C bond in the NpCbl-*c*-COX derivatives upon rotation of the *c* side chain about the C7−C37 bond or upon increasing the steric bulk of X might suggest that downward flexing of the corrin ring is the less energetically costly response to steric interactions between acetamide side chains and the Np ligand on the β face. If such downward flexing does indeed occur and increases with increasing steric bulk of X, the steric interactions between all three of the upward projecting acetamides and the Np ligand, and hence the restriction of side chain rotational freedom by the Np ligand, would be decreased. This could lead to a serious underestimation of the maximum effect of *c* side chain rotational restriction on the ground state entropic destabilization of NpCbl. Inspection of the thermodynamic data in Table 3 for the base-off/on reaction of the NpCbl-c-COX complexes shows that, with the exception of the monocarboxylate, there is a monotonic decrease in K_{meas}, the equilibrium constant for formation of the base-on species, as the X substituent is increased in size.[62] As a result of this possibility, the estimate of 5.6 cal mol^{-1} K^{-1} of entropic destabilization due to maximal restriction of *c* side chain thermal mobility must again be considered as a lower limit.

The question of whether AdoCbl-dependent enzymes use corrin ring side chain entropy to help drive C−Co bond homolysis clearly requires further study. The activation pa-

(58) Saebo, S.; Radom, L.; Schaefer, H. F. *J. Chem. Phys.* **1983**, *78*, 845.

(59) (a) Lenhert, P. G.; Hodgkin, D. C. *Nature (London)* **1961**, *192*, 937. (b) Lenhert, P. G. *Proc. R. Soc. London Ser. A* **1968**, *303*, 45.

(60) (a) Savage, H. F. J.; Lendley, P. F.; Finney, J. L.; Timmins, P. A. *Acta Cryst.* **1987**, *B43*, 280. (b) Bouquiere, J. P. *Physica* **1992**, *B180*−181, 745. (c) Bouquiere, J. P.; Finney, J. L.; Lehmann, M. S.; Lendley, P. F.; Savage, H. F. J. *Acta Cryst.* **1993**, *B49*, 79.

(61) Brodie, J. D. *Proc. Natl. Acad. Sci. U.S.A.* **1969**, *62*, 461.

(62) There is also some suggestion of such downward flexing of the corrin ring from the molecular mechanics calculations. Thus, in NpCbl-*c*-NHiPr, the corrin ring upward fold angle (defined[63] as the angle between the least squares plane including N21, C4, C5, C6, N22, C9, and C10, and that including N24, C16, C15, C14, N23, C11, and C10) decreases from about 7.5° when the *c* side chain points outward ($\omega_1 = \pm 180°$) to about 3.7° when the *c* side chain points toward the Np ligand ($\omega_1 = 0-60°$). For NpCbl-*c*-COO$^-$, the minimum fold angle (at $\omega_1 = 0-60°$) is about 4.2°. Whether or not such small differences in corrin ring fold angle significantly effect the steric interactions between the acetamide side chains and the β alkyl ligand is unclear.

(63) Glusker, J. P. in *B_{12}*, Dolphin, D., Ed.; Wiley: New York, 1982; Vol. 1, pp 23−106.

rameters for enzyme-induced AdoCbl homolysis are unknown since the kinetics of this process have only been studied at a single temperature.[16,17] Thus, the extent to which enzyme-induced homolysis is entropically and enthalpically driven is not known. Furthermore, a recent report[64] of the X-ray crystal structure of the complex of CH_3Cbl with a binding domain fragment of the enzyme methionine synthase surprisingly shows that the axial dimethylbenzimidazole ligand is not coordinated to cobalt in this complex in which the Co axial ligand is instead a histidine residue from the protein. In addition, Kräutler et al.[65] have recently reported the X-ray crystal structure of *Coβ*-cyanoimidazolylcobamide, a CNCbl analog in which the axial dimethylbenzimidazole is replaced by an imidazole ligand. In this analog, the corrin ring has a smaller upward fold than CNCbl itself. This suggests that for methionine synthase at least, absent other effects of protein interactions on the corrin ring conformation, the corrin ring of protein-bound CH_3Cbl may be less upward folded than that of free CH_3Cbl. Unfortunately, the X-ray structure of the methionine synthase fragment−CH_3-Cbl complex is not at sufficiently high resolution to answer this question directly.[66] In addition, the relevance of this binding mode for methionine synthase, which catalyzes the heterolytic formation and cleavage of the C−Co bond of CH_3Cbl, to the AdoCbl-dependent enzymes, which catalyze C−Co bond homolysis, is not clear.[68] While Drennan et al.[64] argue that a common histidine binding motif also occurs in the sequences of human methylmalonyl-CoA mutase and the small subunit of a bacterial glutamate mutase, two AdoCbl-dependent enzymes for which sequence information is available, the actual extent of homology between the methionine synthase fragment and the putative Cbl-binding domains of these two enzymes appears to be quite small. In addition, it is certainly possible that other interactions between the protein and the corrin and/or its substituents in the AdoCbl-dependent enzymes can cause significant changes in corrin ring conformation. Clearly, the answers to these questions require investigations of the interactions of the AdoCbl-dependent enzymes themselves with AdoCbl.

Acknowledgment. This research was supported by the National Institute of General Medical Sciences through Grant GM 48858, the National Science Foundation EPSCoR program through Grant EHR 9108767, the State of Mississippi, and Mississippi State University.

Supplementary Material Available: Table SI, giving tentative ^{13}C NMR assignments for CNCbl-*c*-COO^-, CNCbl-*c*-NMe_2, and CNCbl-*c*-NHiPr and unambiguous ^1H and ^{13}C NMR assignments for CNCbl-*c*-NHMe, Table SII, showing the amide ^1H and ^{15}N chemical shifts of the CNCbl-*c*-COX derivatives, Table SIII, giving the COSY, ROESY, HOHAHA, and HMBC NMR connectivities of CNCbl-*c*-NHMe, Table SIV, giving tentative ^{13}C NMR assignments for the dicyano derivatives of the $CN(H_2O)Cbi$-*c*-COX^+ derivatives, and Table SV giving tentative ^{13}C NMR assignments of the NpCbi-*c*-COX derivatives (14 pages). Ordering information is given on any current masthead page.

IC941084D

(64) Drennan, C. L.; Huang, S.; Drummond, J. T.; Matthews, R. G.; Ludwig, M. L. *Science* **1994**, *266*, 1669.
(65) Kräutler, B.; Konrat, R.; Stupperich, E.; Färber, G.; Gruber, K.; Kratky, C. *Inorg. Chem.* **1994**, *33*, 4128.
(66) In the refinement of the X-ray structure of the complex of CH_3Cbl with the methionine synthase binding domain fragment, the corrin ring coordinates were essentially fixed at those of Rossi et al.,[55] for free CH_3Cbl.[67]
(67) Ludwig, M. L. Personal communication.
(68) Stubbe, J. *Science* **1994**, *266*, 1663.